Comparison of various parametrizations of the double-humped fission barrier

B. S. Bhandari and M. Khaliquzzaman*
Physics Department, Faculty of Science, University of Garyounis, Benghazi, Libya
(Received 19 July 1990)

The double-humped potential barriers in actinide nuclei in the fission direction have been parametrized using three different procedures, namely, the smoothly joined parabolic segments, third-degree polynomials passing through and with zero slopes at the successive extremum points, and straight-line segments connecting the successive extremum points. The fission penetrabilities through the barriers and the ground-state spontaneous fission half-lives for a wide variety of 25 actinide nuclides have been calculated for these different parametrizations. Our results clearly indicate that while the third-degree polynomial and the straight-line parametrizations of the double-humped fission barrier lead to approximately similar results on the fission penetrability and fission half-lives, the corresponding results using the smoothly joined parabolic segment parametrization differ significantly by almost two to five orders of magnitude depending on the specific type of the fissioning nucleus and on the parameters of its corresponding double-humped fission barrier.

I. INTRODUCTION

Most of the actinide nuclei are now known to exhibit a double-humped potential barrier against fission. The shell correction method, developed by Strutinsky,[1] first clearly showed that such fission barriers occur mainly as a result of the superimposition of the oscillatory "shell corrections" or the so-called single-particle effects on the relatively flat potential-energy surfaces predicted by the liquid-drop model in the corresponding deformation regions for the actinide nuclei. The relatively flat or the gently varying macroscopic potential surface arises from the near cancellations between the Coulomb and the surface-energy contributions to the liquid-drop potential energy. Minima and maxima in the total potential-energy surface, when the microscopic shell and pairing corrections have been included, can be traced back to the gaps or concentrations of the single-particle levels at particular deformations. Such gaps and bunchings in the single-particle spectra develop at large deformations, particularly for the spheroidal shapes with special symmetry such as those with major to minor axes ratios of 2 to 1. It is these shell effects that give rise to the second minimum in the potential-energy surface associated with the spontaneous fission isomerism. The concept of the double-humped fission barrier has been spectacularly successful in explaining a host of experimentally observed phenomena such as narrow and broad resonance structures in sub-barrier fission cross sections, fission isomers, and the so-called "isomeric shelf" observed in the deep sub-barrier photofission cross sections of the various actinide nuclei. The theoretical foundation of the double-humped barrier, its experimentally observable consequences, and the various experimental evidences supporting such a two-peaked character of the fission barrier in the actinide nuclei have been extensively reviewed by several authors.[2-5]

The concept of the double-humped fission barrier is essential in understanding simultaneously the low-energy fission cross sections and the various fission half-lives in terms of the penetrability through such a potential barrier. The shape isomers are commonly interpreted as the lowest state of the intermediate minimum, or the so-called second well, between the two barriers of the double-humped fission potential shapes in the actinide nuclei. The competition between the spontaneous fission and the gamma decay to the ground state of the fissioning compound nucleus (first well) from the shape-isomeric state can then be described in terms of the relative penetrabilities through the outer and the inner barriers, respectively, of the double-humped potential shapes at the isomeric energy E_i. On the other hand, the fission barrier as a whole determines the ground-state spontaneous fission half-life of such actinide nuclei. The ability to calculate fission half-lives is essential for theoretical predictions concerning the stability and synthesis of heavy nuclei. Such calculations[6-11] require the detailed knowledge of the variation of the inertial-mass parameter (nuclear inertia) and of the shape of the fission barrier as a function of the fission coordinate along a selected one-dimensional path through the multidimensional potential-energy surface. This path begins at the nuclear ground state and includes saddle points and minima in the fission direction and a few points beyond the last saddle. The nuclear inertia associated with motion in the fission direction can be either calculated microscopically using the cranking model[7,12-14] or obtained phenomenologically in a semiempirical model.[6,8]

The choice of the exact path between the saddle points and minima along the fission direction is obviously open to considerable ambiguity. This concerns the parametrization of the double-humped fission barrier. One of the methods used in the theoretical calculations[6-11] of the fission half-lives constructs the fission barrier by connecting the successive extrema with third-degree polynomials whose derivatives are made to vanish at both ends. This completely defines the corresponding third-degree polynomial. Another commonly used potential parametriza-

tion of the double-humped fission barrier is in terms of the smoothly joined parabolic segments,[5,15–21] each of which represents either a potential barrier or a potential well as the case may be. The potentials as well as their first derivatives are matched at the joining points between the successive parabolic segments. While both these procedures lead to reasonably realistic and smoothly varying fission barrier shapes, there are considerable differences in the curvatures or the widths of the individual potential segments obtained in these two parametrizations of the double-humped fission barrier. As the calculated fission half-lives and the penetrability through such a barrier depend strongly on both the height and the width of the individual potential segments, it is therefore of interest, and thus the purpose of the present paper, to compare the results on fission barrier shapes, on fission penetrabilities, and on fission half-lives calculated using the above two different potential parametrizations. For comparison purposes, we have also included a third potential parametrization in which the successive extrema are connected by straight lines. While obviously not of much physical interest, such straight lines have been commonly used[8] to construct the later part (beyond the last saddle) of the double-humped fission barrier in the heavy nuclei.

In Sec. II we describe the various potential parametrizations of the double-humped fission barrier and compare the resulting shapes. Sections III and IV deal with the calculation of the fission penetrability and that of the fission half-lives, respectively, within the framework of a double-humped fission barrier model. The formalism of such calculations is briefly described, and the results obtained using the various potential parametrizations are critically compared. A brief discussion of the inertial-mass function is given in Sec. V. Finally, a discussion of the results and the conclusions are presented in Sec. VI.

II. FISSION BARRIER PARAMETRIZATION

A. Formalism

The double-humped fission barrier (Fig. 1) to be parametrized consists of a primary potential well (I) containing the ground state of the spontaneously fissioning nucleus, and a second well (II) flanked by a barrier on each side. The barrier to the left (A) of the second well is usually termed the "inner barrier" while that to the right (B) of the second minimum is called the "outer barrier" in fission literature. In order to compare the results of various parametrizations of such a potential barrier, we have considered three different types of such potential parametrizations and the details are given in the following.

1. Using smoothly joined parabolic segments

The potential barrier has been parametrized in this case by smoothly joining four parabolas and is given as a function of the dimensionless deformation parameter (fission coordinate) ϵ by[16]

$$V(\epsilon)=E_j\pm\tfrac{1}{2}\mu\omega_j^2(\epsilon-\epsilon_j)^2 , \tag{1}$$

where the positive sign applies for $j=0$ and 2, and the negative sign for $j=1$ and 3. E_j represent the minima and maxima of the potential, $\hbar\omega_j$ their respective curvature energies, and ϵ_j the locations of the extrema on the deformation (fission coordinate) axis. μ is the inertial-mass parameter of the fissioning nucleus along the ϵ direction and has been assumed to be constant for all values of ϵ. Since the deformation parameter ϵ is dimensionless, μ has the dimensions of the moment of inertia. The value of μ used in the present work has been taken to be equal to[16]

$$\mu=0.054\,A^{5/3}\hbar^2\ \text{MeV}^{-1} , \tag{2}$$

where $\hbar$ is to be expressed in MeV sec and A is the nuclear mass number.

The potential barrier defined by Eq. (1) is seen to contain a total of twelve parameters, three to describe each of the four parabolas. We require that the parabolas representing the inner and the outer barriers join smoothly with the parabolas representing the primary and the intermediate (second) minima at their points of intersection. This means that the potentials $V(\epsilon)$ as well as their first derivatives must be matched at the points of intersection. This leads to six matching conditions or equations. Three of these determine the locations of the points of intersection on the ϵ axis and the remaining three help eliminate three of the twelve parameters required in Eq. (1). Another parameter is eliminated by the translational invariance of the potential barrier on the ϵ axis, by arbitrarily setting

$$V(\epsilon)=E_0, \quad \text{at } \epsilon=\epsilon_0=0 . \tag{3a}$$

This reduces the number of parameters required to specify the double-humped fission barrier to eight. These are chosen to be the four energies E_0, E_1, E_2, and E_3 and the four curvature energies $\hbar\omega_0$, $\hbar\omega_1$, $\hbar\omega_2$, and $\hbar\omega_3$. The exact locations of the various extrema as well as of the points of intersection of the successive parabolic segments along the ϵ axis can then be expressed[16–19] in terms of these eight basic parameters. The double-humped fission barrier parametrized in this manner in terms of four smoothly joined parabolic segments has a zero slope (first derivative) at the origin as well as at all its other extrema (maxima or minima). At the origin ($\epsilon=\epsilon_0=0$), we further require

$$V(\epsilon)=E_0=-\tfrac{1}{2}\hbar\omega_0 , \tag{3b}$$

such that the ground-state energy, $E_g=E_0+\frac{1}{2}\hbar\omega_0$, in the primary potential well of the spontaneously fissioning nucleus is equal to zero. The value of the curvature energy $\hbar\omega_0$ of the primary potential well has been assumed equal to 1 MeV for all the actinide nuclides considered in the present work.

Information concerning the parameters E_1, E_3 and $\hbar\omega_1$, $\hbar\omega_3$ is usually obtained by analyzing the measured energy dependence of the near-barrier fission cross sections of the actinide nuclei. On the other hand, the experimental information on the isomeric energies and on the isomeric-decay half-lives help determine E_2 and $\hbar\omega_2$ in conjunction with other observed characteristics such

as the vibrational resonances in the sub-barrier fission cross sections and the so-called "isomeric shelf," if observed in a given nucleus. It is important to realize, however, that most of the experimental information used in extracting these parameters comes from near the top of the barriers and from the isomeric excitation energy. The heights of the fission barriers thus estimated are reasonably reliable. However, extrapolating the same values of the parameters $\hbar\omega_j$ from those near the top of the barriers down to much lower excitations and in deformation regions far from their corresponding extrema (maxima or minima) is open to question in view of the absence of any compelling physical reasons suggesting that the shape of the double-humped fission barrier must be exactly quadratic in the entire range of the deformations involved during the fission process. One of the present authors[22] has recently attempted to test the adequacy of using smoothly joined parabolic segments to parametrize the double-humped fission barrier by examining its simultaneous consistency with the three relevant fission observables, namely, the near-barrier fission cross sections, isomeric half-lives and their fission branching ratios, and the ground-state spontaneous fission half-lives for a wide variety of a total of 25 actinide nuclides. The results of such a systematic analysis suggest that such a parametrization is quite adequate at least for the even-even nuclei as it reproduces satisfactorily the various observed fission characteristics. Major difficulties remain, however, for the odd-mass and for the doubly odd nuclei where the calculated ground-state spontaneous fission half-lives are found to be several orders of magnitude larger than those measured.

2. *Using third-degree polynomials*

A simple spline method is used to parametrize the double-humped fission barrier in this case by connecting the successive extremum points with a third degree polynomial. The potential energy as a function of the dimensionless deformation parameter (ϵ) in the energy region between two successive extrema is given as

$$V_j(\epsilon)=A_{j0}+A_{j1}\epsilon+A_{j2}\epsilon^2+A_{j3}\epsilon^3,\quad \epsilon_{j-1}\le\epsilon\le\epsilon_j\ ,\quad j=1,2,3,4\ . \tag{4}$$

The potential barrier as defined by Eq. (4) in the region between two successive extremum points is seen to contain four parameters A_{jk}, $k=0$, 1, 2, and 3 for a given value of j. Two of these parameters are determined by specifying the exact values of $V_j(\epsilon)$ at the supposedly known values of the two extremas ϵ_j on the ϵ axis. The remaining two parameters are determined by requiring that the third-degree polynomial must have zero slopes at the two extremas:

$$dV_j(\epsilon)/d\epsilon=A_{j1}+2A_{j2}\epsilon+3A_{j3}\epsilon^2=0\ ,\quad \text{at } \epsilon=\epsilon_{j-1},\ \text{and at } \epsilon=\epsilon_j\ . \tag{5}$$

This completely defines the third-degree polynomial between two successive extremum points. The entire double-humped fission barrier is then parametrized in this manner by connecting successive extremum points with such third-degree polynomials. The double-humped fission barrier obtained using such a procedure exhibits zero slopes at the origin as well as at all its other extremas. However, it also has a zero slope at the point of emergence (exit point) of the spontaneously fissioning nucleus from the corresponding double-humped fission barrier. As the exit point is not one of the extremum points of the fission barrier, it seems physically unreasonable and incorrect to require a zero first derivative of the potential $V_j(\epsilon)$ at this point. In the present work we have therefore considered two different variations of such a third-degree polynomial parametrization which differ in their slopes at the exit point, and thus lead to different potential shapes for the last part (beyond the second saddle) of the corresponding double-humped fission barriers.

(i) In the first such variation, termed as the third-degree polynomials (a), we require that the potential energy $V_j(\epsilon)$ has the same slope as that of the parabolic parametrization at the final exit point (ϵ_4). Thus, for $j=4$, we require that

$$dV_j(\epsilon)/d\epsilon=-\mu\omega_3^2(\epsilon_4-\epsilon_3),\quad \text{at } \epsilon=\epsilon_4\ . \tag{5a}$$

Such a requirement leads to the potential shape obtained in the third-degree polynomial (a) parametrization exactly coincident with that of the parabolic parametrization in the region between the second saddle (ϵ_3) and the final exit point (ϵ_4) as shown by curve *a* in Figs. 1 and 2.

(ii) In the second such variation, termed as the third-degree polynomials (b), we replace the last part of the fission barrier in the third-degree polynomial parametrization by a straight line connecting the second saddle (ϵ_3) and the final exit point (ϵ_4). Thus, for $j=4$ in Eq. (4), we require that

$$A_{j3}=A_{j2}=0 \quad \text{and} \quad A_{j1}=-A_{j0}/\epsilon_4=-E_3/(\epsilon_4-\epsilon_3)\ . \tag{5b}$$

Such a requirement leads to the potential shape obtained in the third-degree polynomials (b) parametrization exactly coincident with that of the straight-line parametrization in the region between the second saddle and the final exit point as shown by curve *b* in Figs. 1 and 2.

As mentioned earlier, such third-degree polynomial parametrizations with a straight line representing the last part of the fission barrier (beyond the second saddle) have already been considered in the past in fission literature by several authors.[7,8] There is, however, a slight difference. While we have constructed the last part of the barrier by a straight line connecting the second saddle with the final exit point as obtained in the parabolic parametrization in the present work, these authors[7,8] use a straight line from the second saddle through a point somewhat beyond the exit point at the bottom of the valley that leads towards scission. While such a choice somewhat beyond the exit point might help reproduce the observed spontaneous fission half-life of a given nucleus, it also introduces an arbitrariness and ambiguity in the parametrization in particular when we wish to compare the results obtained using the various parametrizations of the fission barrier.

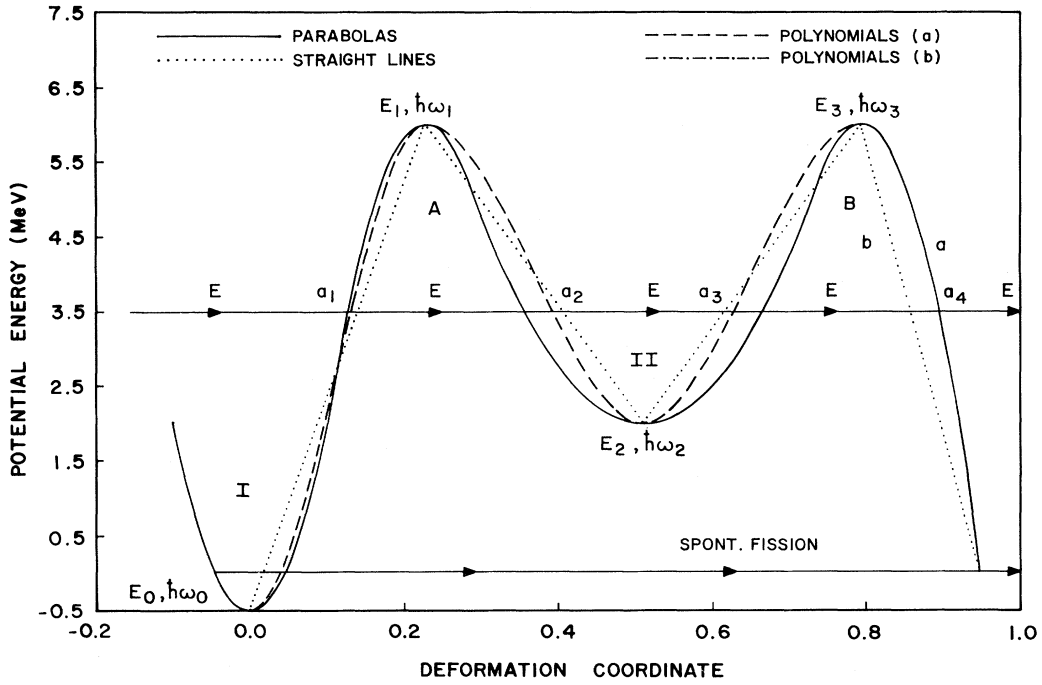

FIG. 1. Symmetric double-humped fission barriers parametrized as per the various different procedures described in the text. The barrier parameters of the smoothly joined parabolic segment potential are $E_0=-0.5$ MeV, $\hbar\omega_0=1.0$ MeV, $E_1=6.0$ MeV, $\hbar\omega_1=1.0$ MeV, $E_2=2.0$ MeV, $\hbar\omega_2=0.5$ MeV, $E_3=6.0$ MeV, $\hbar\omega_3=1.0$ MeV. Curves a and b beyond the second saddle also correspond to the third-degree polynomials (a) and (b), respectively, as discussed in the text.

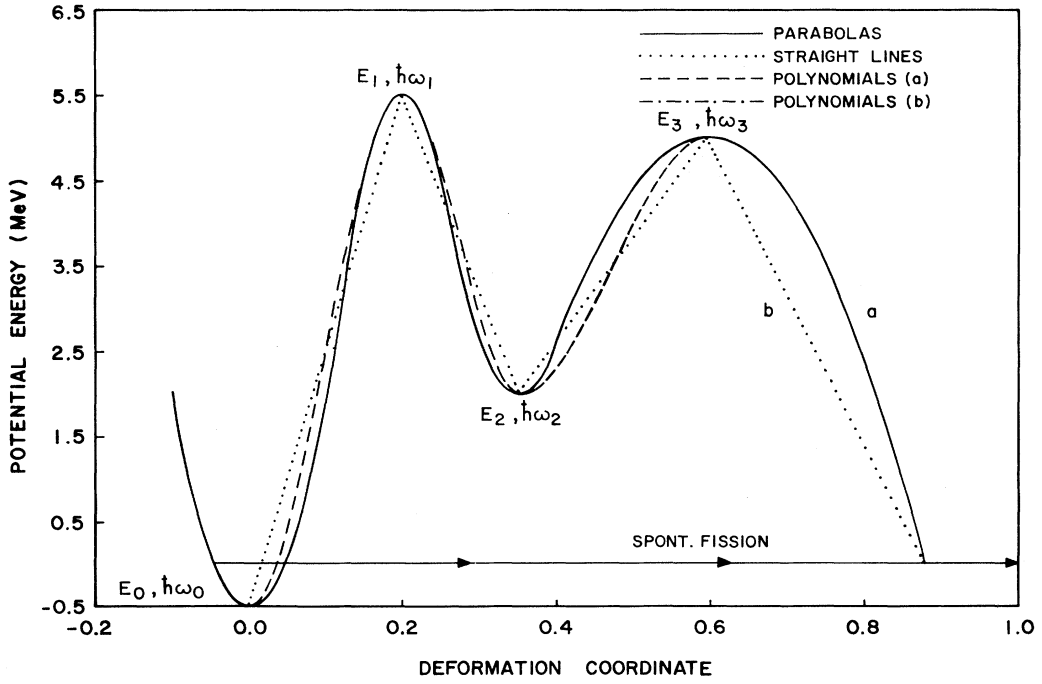

FIG. 2. Asymmetric double-humped fission barriers parametrized as per the various different procedures described in the text. The barrier parameters of the smoothly-joined parabolic segment potential are $E_0=-0.5$ MeV, $\hbar\omega_0=1.0$ MeV, $E_1=5.5$ MeV, $\hbar\omega_1=1.25$ MeV, $E_2=2.0$ MeV, $\hbar\omega_2=1.0$ MeV, $E_3=5.0$ MeV, $\hbar\omega_3=0.5$ MeV. Curves a and b beyond the second saddle have the same meanings as in Fig. 1.

The above parametrizations of the double-humped fission barrier in terms of the third-degree polynomials require an exact knowledge of the various extremum points on the fission potential-energy surfaces both along the energy as well as along the deformation axes. While the measured data on the near-barrier fission cross sections and on the fission isomers can be used to obtain information concerning the positions of the various extremum points along the energy axis, the fission experiments do not yet provide any conclusive information at all on the exact locations of these extremum points along the deformation axis. This type of potential parametrization has therefore been considered so far only in theoretical calculations of the fission barrier as a one-dimensional path through the calculated[6-11] multidimensional potential-energy surface. In such calculations the positions of the various extremum points are determined both along the energy as well as along the deformation axes. In the present work the values of the deformation coordinate at various extremum points are obtained from the parabolic parametrization as explained in detail in Sec. II B.

3. *Using straight lines*

In such a parametrization, the potential energy between two successive extremum points is given as a function of the dimensionless deformation parameter (ϵ) as

$$V_j(\epsilon)=A_{j0}+A_{j1}\epsilon, \quad \epsilon_{j-1}\leq\epsilon\leq\epsilon_j \ , \quad j=1,2,3,4 \ . \tag{6}$$

The potential barrier as defined by Eq. (6) in the region between two successive extremum points is seen to contain two parameters, A_{j0} and A_{j1}, for a given value of j. These two parameters are determined by specifying the exact values of $V_j(\epsilon)$ at the supposedly known values of the two extremum points ϵ_j on the ϵ axis. This completely defines the above parametrization.

Such a potential parametrization is obviously not of much physical interest. The fission barrier obtained in such a parametrization does not exhibit a zero slope at the origin and is thus physically unreasonable for the calculation of the ground-state spontaneous fission half-lives. Besides, it also requires an exact knowledge of the various extremum points both along the energy as well as along the deformation axes, and thus suffers from the same limitations as discussed above for the third-degree polynomial parametrization. It is intuitively simple, however, and we have therefore also included this parametrization of the double-humped fission barrier in the present work in order to investigate the range of deviations between the calculated fission penetrabilities and fission half-lives through more realistic and smoothly varying fission barrier shapes, and those calculated through such simple though unrealistic potential shapes parametrized by connecting the successive extremum points with straight lines.

B. Results

Having outlined the basic formalism underlying the above various different parametrizations of the double-humped fission barriers, we now compare a sample each of the shapes obtained using such procedures. For a given set of the barrier parameters (E_j and $\hbar\omega_j$, $j=0,1,2,3$) required for the smoothly joined parabolic parametrization, we first obtain a complete set of the numerical values of $V(\epsilon)$ in the complete range of the deformation parameter ϵ spanning the entire double-humped fission barrier. From this complete set of numerical values of $V(\epsilon)$ vs ϵ, we obtain the exact locations of all the relevant extremum points both along the energy as well as along the deformation axes. These data then become the input for the other two potential parametrizations, i.e., using the third-degree polynomials and using the straight lines. Beyond the second saddle, we define the so-called exit point along the deformation axis where the potential energy $V(\epsilon)$ falls to a value equal to the ground-state energy of the fissioning nucleus. This is the point where the spontaneously fissioning nucleus is supposed to emerge from the corresponding double-humped fission barrier. As the ground-state energy E_g of the fissioning nucleus in the primary potential well has been assumed to be equal to zero in the present work, we require that

$$V(\epsilon)=0 \quad \text{at } \epsilon=\epsilon_4 \ . \tag{7}$$

This then completely defines the shape of the entire double-humped fission barrier.

Figures 1 and 2 show the comparison of such suitably parametrized shapes passing through the same extremum points for a symmetric and for an asymmetric double-humped fission barrier, respectively. The parameters of these double-humped fission barriers are taken from those given originally by Cramer and Nix in their[16] smoothly joined parabolic segment parametrization of such a potential barrier. Some of the important features of such comparisons can be summarized as follows.

(1) The shapes corresponding to the parametrizations using the third-degree polynomials and those using the straight lines seem to lie fairly close to each other in the entire range of the deformation coordinate except for the last part of the barrier (beyond the second saddle) where the shape obtained in the third-degree polynomials (a) parametrization is seen to be coincident with the corresponding parabolic segment. Also, as expected, the potential shape in the third-degree polynomials (b) parametrization is seen to be exactly coincident with that of the straight-line parametrization in this region of the deformation coordinate. Otherwise, the polynomials are seen in general to be somewhat below the straight lines in deformation regions close to the bottom of the barriers, both near the ground state and also near the isomeric minimum. On the other hand, the polynomials are seen to be somewhat above the straight lines in deformation regions close to the top of the barriers. Such similarity in the potential shapes should then lead to approximately similar values of the calculated fission penetrability and of the fission half-lives through the corresponding double-humped barriers.

(2) Both of these above shapes differ noticeably from the potential shape obtained using the smoothly joined parabolic parametrization. Except for the cases where

the barrier peaks are very narrow (larger values of $\hbar\omega_1$ and $\hbar\omega_3$), the individual parabolic segments in the barrier regions are seen to be relatively broader as compared with the shapes obtained using the third-degree polynomials as well as the straight lines in the corresponding deformation regions. Such differences are also seen to become more pronounced as the individual barrier segments become wider (smaller values of $\hbar\omega_1$ and $\hbar\omega_3$). These features will correspondingly affect the calculated values of the fission penetrability and of the fission half-lives through such potential shapes. In Fig. 1 the parabolic shapes appear relatively narrower in the barrier regions because of the relatively much broader second well (smaller value of $\hbar\omega_2$), and due to the consequent shift of the points along the deformation axis where the corresponding parabolic segments join smoothly.

(3) A comparison of the above parametrized shapes in the second-well region also shows features similar to those obtained in the barrier regions. For very narrow second-well regions (large $\hbar\omega_2$), the various parametrized shapes are nearly coincident with each other, and appear very similar. However, as the width of the second-well region increases (smaller $\hbar\omega_2$), the parabolic shape tends to become broader as compared to the shapes obtained in the other two parametrizations. This is clearly evident for the symmetric double-humped potential barrier displayed in Fig. 1, where the polynomial and the straight-line parametrized shapes in the second-well region are seen to be much narrower as compared to the shape obtained using the parabolic parametrization. However, the trend is somewhat reversed for the asymmetric double-humped barrier shown in Fig. 2, where the parabolic shape is now seen to be relatively narrower. This has been caused because of the relatively much broader outer-barrier segment in this case. These features arise because of the consequent shift in the relative positions of the points of intersection of the successive parabolic segments on the deformation axis in the smoothly joined parabolic parametrization. Such differences in the width of the second well in the various parametrized shapes of the double-humped fission barrier will then lead to corresponding changes in the energies of the quasibound states in the second minimum. For example, a narrower shape in the second-well region shall tend to push up these quasibound states on the energy scale and vice versa. Such quasibound states are known to manifest themselves in the form of narrow resonances in the sub-barrier fission penetrability through a double-humped potential barrier.

(4) The differences in such parametrized shapes near the top of the barriers will be expected to lead to noticeable differences in the slopes of the near-barrier fission penetrability. Narrower shapes near the top of the barriers should lead[20] to relatively smaller values of such slopes.

(5) Individual potential segments are symmetric about their extremum point in the parabolic parametrization. The slopes of the individual polynomials and straight lines depend, however, on the relative separation of the two successive extremum points. The shapes generated using the polynomial and the straight-line parametrizations will therefore not be always symmetric about the extremum point in the individual potential segments, and may exhibit features similar to those found for a biharmonic oscillator.[23,24]

III. FISSION PENETRABILITY CALCULATION

A. Formalism

The penetrability through the double-humped fission barrier parametrized as per the procedures described in Sec. II has been calculated in the Wentzel-Kramers-Brillouin (WKB) approximation. Details of such penetrability calculations have already been reported in some of our earlier work,[17–22] and, therefore, we only quote here the analytical expression for the penetrability.

Defining P_A, P_B, and P as the respective penetrabilities for the inner barrier (A) alone, outer barrier (B) alone, and the entire double-humped barrier illustrated in Fig. 1, it has been shown[17–22] that

$$P=P_AP_B/(\{1+[(1-P_A)(1-P_B)]^{1/2}\}^2\cos^2\nu_2 + \{1-[(1-P_A)(1-P_B)]^{1/2}\}^2\sin^2\nu_2) , \quad (8)$$

where the individual penetrabilities (P_A and P_B) are given[25] in the WKB approximation as

$$P_A=[1+\exp(2\nu_1)]^{-1} , \quad P_B=[1+\exp(2\nu_3)]^{-1} . \quad (9)$$

The quantities ν_i are the integrals in respective regions, as shown in Fig. 1, of the wave numbers or the momentum functions,

$$K_1(\epsilon)=\{2\mu[E-V(\epsilon)]/\hbar^2\}^{1/2}=iK_2(\epsilon) , \quad (10)$$

for example,

$$\nu_1=\int_{a_1}^{a_2}K_2(\epsilon)d\epsilon , \quad \nu_2=\int_{a_2}^{a_3}K_1(\epsilon)d\epsilon , \quad \nu_3=\int_{a_3}^{a_4}K_2(\epsilon)d\epsilon . \quad (11)$$

The classical turning points a_1, a_2, a_3, and a_4 are as shown in Fig. 1 for an incident energy E. In actual calculations these turning points are obtained analytically for the smoothly joined parabolic and straight-line parametrizations, and found numerically for the third-degree polynomial parametrization using the Newton-Raphson method[26] to obtain the real roots of the equation,

$$[V_j(\epsilon)-E]=0, \quad j=1,2,3,4 . \quad (12)$$

The inertial-mass parameter μ is assumed constant for all values of ϵ, and has the value as given in Eq. (2).

B. Results

In Figs. 3 and 4 we compare the results of our penetrability calculations through such parametrized shapes of

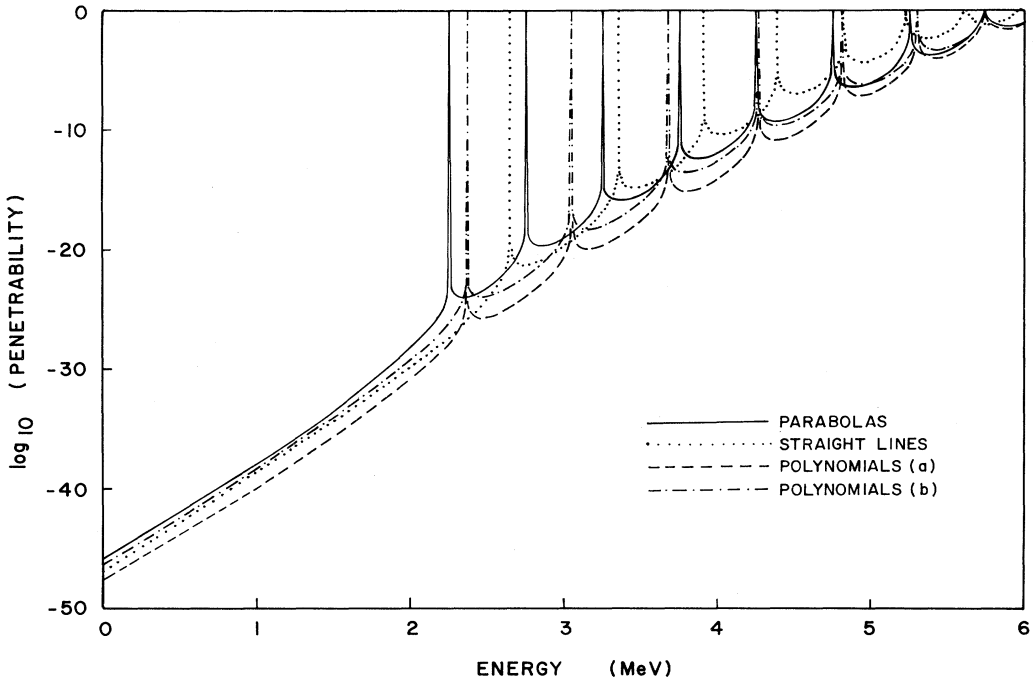

FIG. 3. A logarithmic plot of the fission penetrabilities through the symmetric double-humped fission barriers as parametrized in Fig. 1.

the double-humped fission barriers as displayed earlier in Figs. 1 and 2, respectively. The main features of such comparisons can be summarized as in the following.

(1) The calculated penetrabilities are seen to exhibit narrow subbarrier resonances at energies corresponding to those of the quasibound states in the second well. Such resonances are seen (Fig. 3) to rise to the maximum possible value of unity for the fission penetrability through the symmetric double-humped barriers. For the asymmetric double-humped barriers, however, the pene-

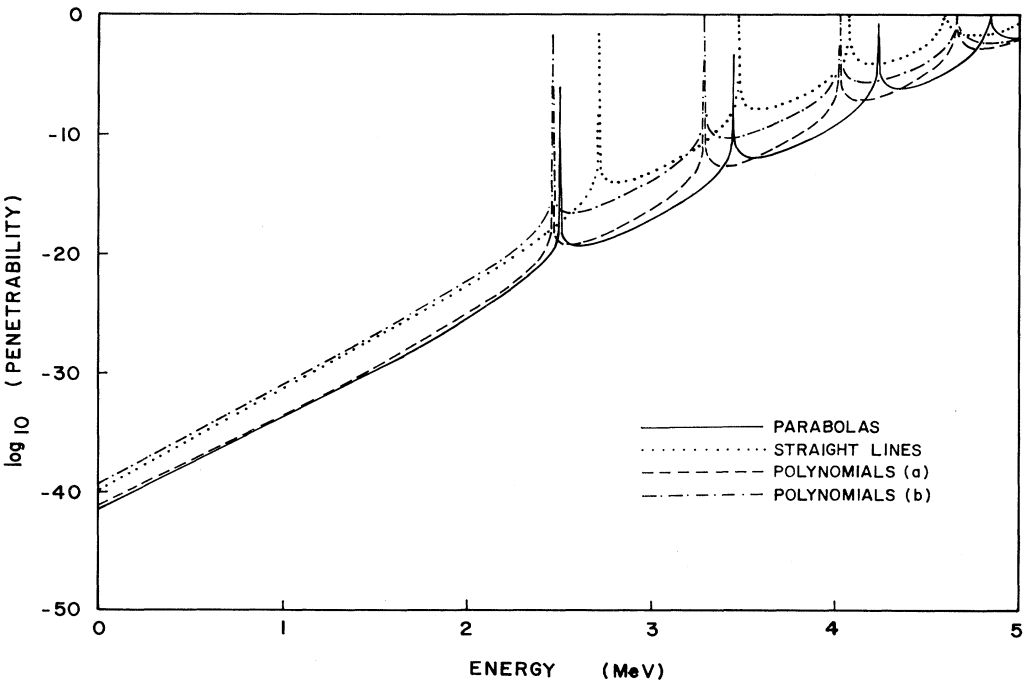

FIG. 4. A logarithmic plot of the fission penetrabilities through the asymmetric double-humped fission barriers as parametrized in Fig. 2.

trability resonances do not seem to rise that high as seen in Fig. 4. Such features of the penetrability through a double-humped fission barrier are already known and well documented in fission literature.[5,16–21]

(2) The behavior of the calculated penetrability as a function of energy can be understood in terms of the various parametrized shapes of the corresponding double-humped fission barriers. For the symmetric double-humped barrier displayed in Fig. 1, we observe that while the parabolic shape is considerably wider in the region of the second well as compared to the corresponding shapes obtained in the other parametrizations, it is also seen to be consistently much lower in height in most of this region. This results (Fig. 3) in a higher penetrability for the parabolic barrier as compared to that for the other parametrizations at energies near the bottom of the double-humped potential barrier. Such a trend is seen to persist up to an energy of about 3 MeV, above which the straight-line parametrization leads to higher penetrability. The lowest penetrability corresponds to the third-degree polynomials (a) parametrization, which exhibits consistently broader inner and outer barriers in Fig. 1. The calculated penetrabilities corresponding to the other two parametrizations are seen to lie between these two extremes. It is interesting to note, however, that the differences in the values of the calculated penetrabilities for the various parametrizations do not seem to exceed two to three orders of magnitude for the symmetric double-humped potential barrier of Fig. 1. While the overall differences in the calculated penetrabilities in various parametrizations of the asymmetric double-humped barrier of Fig. 2 are also of two to three orders of magnitude as seen in Fig. 4, the penetrability values at energies near the bottom of the barrier are now seen to be the lowest for shapes corresponding to the parabolic and the third-degree polynomials (a) parametrizations. This is because of the relatively wider outer barriers obtained in these parametrizations. The other two parametrizations lead to shapes yielding somewhat higher penetrabilities. Such trends are also seen to persist even at higher energies near the top of the outer (and the lower) barrier as evident in Fig. 4. The penetrabilities corresponding to the straight-line parametrization are consistently larger than those for the other shapes at higher energies because of the relatively narrower barrier shapes obtained in such a parametrization near the top of the barriers.

(3) For the symmetric double-humped barrier, the second well is narrower for the polynomial and straight-line parametrizations as compared to that for the parabolic parametrization. Consequently, the quasibound states are pushed up on the energy scale. This is seen clearly in Fig. 3 where the resonances in the penetrability appear at relatively higher energies for the polynomial and straight-line parametrizations than those for the parabolic parametrization. The straight-line parametrization seems to push up the energies of the quasibound states even more than that seen for the polynomial parametrizations. The two different variations of the third-degree polynomial parametrizations considered in the present work differ only in their shapes of the fission barrier beyond the second saddle. This does not affect (Figs. 3 and 4) the positions of the penetrability resonances on the energy scale as these are determined mainly by the shape of the second minimum. The peak values of the penetrability at such coincident resonances shall, however, differ depending on the relative shapes of the corresponding outer barriers. Unfortunately, as the penetrability resonances are very narrow, such differences in the peak values could not be shown explicitly in Figs. 3 and 4.

(4) For the asymmetric double-humped barrier, the second well in the parabolic parametrization seems to be relatively narrower than that in the polynomial parametrization, and relatively wider than that in the straight-line parametrization at energies near the isomeric minimum. This results (Fig. 4) in the low-lying penetrability resonances for the parabolic shape lying in between those for the other two parametrizations. At higher energies, however, the second well with the parabolic shape becomes narrower as compared to both other parametrizations, and consequently the corresponding penetrability resonances are pushed up in energy relative to those for the other two shapes. This is clearly apparent in Fig. 4 at energies greater than 3.5 MeV.

(5) The slope of the fission penetrability at energies near the top of the barrier depends upon the relative widths of the barriers in the corresponding energy region given in terms of the parameters $\hbar\omega_1$ and $\hbar\omega_3$. In general, the wider the barrier, the larger is the rate of variation of the penetrability with energy. This is clearly apparent for the third-degree polynomials (a) parametrization in Fig. 3 in the energy range 5–6 MeV, and for the parabolic parametrization in Fig. 4 at energies close to the top of the outer (and the lower) barrier. Such variations in the slopes of the near-barrier fission penetrability with the change in the values of the barrier parameters $\hbar\omega_1$ and $\hbar\omega_3$ have been discussed in detail in one of our recent publications.[20]

IV. FISSION HALF-LIVES CALCULATION

A. Formalism

Using the model of the double-humped fission barrier parametrization as per the procedures described in Sec. II, we have calculated the ground-state spontaneous fission half-lives and the isomeric half-lives for our static potential shapes with a constant mass parameter with respect to the deformation coordinate. Various limitations of such calculations are discussed in detail in one of our recent papers.[22] The expressions used to compute the various fission half-lives have been taken from the earlier work of Nix and collaborators,[15,16] and are briefly summarized in the following.

1. Spontaneous fission half-life

The spontaneous fission decay half-life from the ground-state level E_g can be written as

$$\tau_{\text{g.s.}}^{\text{SF}} = (\ln 2)(2\pi/\omega_0)[P(E_g)]^{-1} , \tag{13}$$

where ω_0 is the frequency of assault on the fission barrier

taken as 1 MeV/$\hbar$ in the present work, and $P(E_g)$ is the penetrability through the entire double-humped fission barrier at the ground-state energy E_g.

2. *Isomeric half-life*

The total isomeric half-life from the isomeric state in the second well can be written in terms of its partial decay half-lives as

$$(\tau_i)^{-1}=(\tau_i^{\gamma})^{-1}+(\tau_i^{\mathrm{SF}})^{-1} . \tag{14}$$

In this expression, τ_i^{γ} represents the half-life for the gamma decay from the isomeric state to the ground state (in the first well) of the fissioning compound nucleus. This is a two-step process: first, the tunneling through the inner barrier at energy E_i and subsequently the electromagnetic deexcitation to the ground state of the fissioning nucleus. An empirical relation obtained earlier by Nix and Walker[15] for this decay half-life is given as

$$\tau_i^{\gamma}\cong 10^{-14}[P_A(E_i)]^{-1}\ \mathrm{sec} , \tag{15}$$

where $P_A(E_i)$ is the penetrability through the inner barrier at energy E_i.

The spontaneous fission decay half-life from the isomeric state E_i, denoted as τ_i^{SF} in Eq. (14), depends only on the tunneling through the outer barrier, and can be written as

$$\tau_i^{\mathrm{SF}}=(\ln 2)(2\pi/\omega_2)[P_B(E_i)]^{-1} , \tag{16}$$

where ω_2 is the frequency of assaults on the outer barrier, taken to be of the order of 1 MeV/$\hbar$ as listed in Table II for most of the nuclei considered in the present work. $P_B(E_i)$ is the penetrability through the outer barrier at energy E_i. The various penetrabilities (P_A, P_B, and P) have been calculated in the present work in the WKB approximation as described in Sec. III.

B. Results

The results of the fission half-lives calculations using the above four parametrizations of the corresponding double-humped fission barrier for a wide variety of 25 actinide nuclei are displayed in Tables I and II. Table I compares the parameters of the double-humped fission barriers parametrized by smoothly joined parabolic segments for such nuclei with those recommended in fission literature. This table has been reproduced from one of our recent works in which Bhandari[22] has examined the adequacy of such a parametrization. However, there is a slight difference in the potential parametrization in our earlier work[22] and the present investigation. The double-humped fission barrier was parametrized in our earlier work in terms of the three smoothly joined parabolic segments, and a constant value of $\omega_0=1$ MeV/$\hbar$ was used for the assault frequency to compute the ground-state spontaneous fission half-lives for the various actinide nuclei. In the present investigation we have parametrized the double-humped fission barrier in terms of four smoothly joined parabolic segments thus including explicitly the parabolic segment corresponding to the primary potential well containing the ground state of the spontaneously fissioning nucleus. Such parametrized shapes of the double-humped fission barrier exhibit zero slopes (first derivative) at the origin, and appear physically more reasonable for the calculation of the ground-state spontaneous fission half-lives. The curvature energy parameter ($\hbar\omega_0$) corresponding to the primary potential well has been given the same constant value equal to 1 MeV for all the 25 actinide nuclides considered in the present work. A comparison of the calculated values of the ground-state spontaneous fission half-lives obtained in our earlier work[22] and those listed for the parabolic parametrization in Table II reveals that the fission barrier parametrized in terms of four smoothly joined parabolic segments consistently leads to slightly higher values than those obtained using three smoothly joined parabolas. However, the differences in the calculated values for the two such parametrizations do not exceed a factor of five for any of the nuclides listed, and are thus well within one order of magnitude.

For these sets of parameters (Table I) of the double-humped fission barrier, we have determined the exact locations of the various extremum points both along the energy as well as along the deformation axes in the smoothly joined parabolic parametrization. Using these sets of data on the various relevant extremum points, we have then parametrized the barrier shapes using the third-degree polynomials, and also using the straight lines to connect the successive extrema along the deformation axis. Such parametrized shapes of the double-humped fission barrier have then been used to compute the fission half-lives of various actinide nuclei as described earlier.

The results of penetrability calculations discussed earlier in Sec. III B clearly indicate that the quasibound states in the second well appear at somewhat different energies in the above three potential parametrizations. Such changes in the isomeric energy (ground state in the second well) lead to considerable differences in the isomeric half-lives. As these effects tend to overlap with the differences in half-lives caused by the differently parametrized potential shapes, it does not seem very meaningful to compare the calculated results on the isomeric half-lives in the various potential parametrizations. No such difficulty arises for the ground-state spontaneous fission half-life calculations, however, and thus the results of such calculations for a wide variety of a total of 25 actinide nuclei are compared in Table II.

We observe that the calculated ground-state spontaneous fission half-lives for most of the actinide nuclides listed in Table II are within one order of magnitude of each other when obtained using the third-degree polynomials (b) and the straight-line parametrizations. However, these results are smaller by almost two to five orders of magnitude than those calculated using the parabolic and the third-degree polynomials (a) parametrizations. Such differences are seen to be the smallest for the even-even nuclei and the largest for the doubly-odd nuclides. We further observe that the values of the calculated fission half-lives using the parabolic parametrization are much closer to those obtained using the third-degree polynomials (a) parametrization than in the third-degree polynomi-

als (b) parametrization.

As the two commonly used methods of parametrizing the double-humped fission barrier in the recent fission literature are those using the parabolic and the third-degree polynomials (b) parametrizations, it is of interest to compare the results of the calculated ground-state spontaneous fission half-lives of a variety of the actinide nuclides using such procedures. We observe that for all

TABLE I. Comparison of the double-humped fission barrier parameters (Ref. 22) for the 25 actinide nuclides used in the present work with those recommended by Bjørnholm and Lynn (Ref. 5). For the primary potential well the parameters $E_0 = -0.5$ MeV and $\hbar\omega_0 = 1.0$ MeV have been assumed for all the nuclides listed.

Compound nucleus Even-odd (Z-N)	Source of the barrier parameters	Double-humped fission barrier parameters E_1 (MeV)	E_2 (MeV)	E_3 (MeV)	$\hbar\omega_1$ (MeV)	$\hbar\omega_2$ (MeV)	$\hbar\omega_3$ (MeV)
^{236}U	Present work	5.63	2.27	5.53	1.04	0.70	0.60
(*e-e*)	Recommended	5.6±0.2		5.5±0.2	1.04		0.60
^{238}U	Present work	5.90	2.06	5.60	1.04	1.00	0.60
(*e-e*)	Recommended	5.7±0.2		5.7±0.2	1.04		0.60
^{237}Np	Present work	5.70	2.40	5.40	0.80	1.00	0.52
(*o-e*)	Recommended	5.7±0.2		5.4±0.2	0.80		0.52
^{235}Pu	Present work	5.80	2.10	5.10	0.80	1.00	0.52
(*e-o*)	Recommended			5.1±0.4	0.80		0.52
^{237}Pu	Present work	5.90	2.10	5.20	0.80	1.00	0.52
(*e-o*)	Recommended	5.90		5.20	0.80		0.52
^{238}Pu	Present work	5.60	2.03	5.00	1.04	1.00	0.60
(*e-e*)	Recommended	5.5±0.2		5.0±0.2	1.04		0.60
^{239}Pu	Present work	6.00	2.20	5.65	0.80	1.00	0.52
(*e-o*)	Recommended	6.2±0.2		5.5±0.2	0.80		0.52
^{240}Pu	Present work	5.57	1.90	5.07	1.04	1.00	0.60
(*e-e*)	Recommended	5.6±0.2		5.1±0.2	1.04		0.60
^{241}Pu	Present work	6.10	1.70	5.25	0.80	1.00	0.52
(*e-o*)	Recommended	6.1±0.2		5.4±0.2	0.80		0.52
^{242}Pu	Present work	5.50	1.95	5.10	1.04	1.00	0.60
(*e-e*)	Recommended	5.6±0.2		5.1±0.2	1.04		0.60
^{243}Pu	Present work	5.70	1.95	5.00	0.80	1.00	0.52
(*e-o*)	Recommended	5.9±0.2		5.2±0.2	0.80		0.52
^{244}Pu	Present work	5.55	2.05	5.00	1.04	1.00	0.60
(*e-e*)	Recommended	5.4±0.2		5.0±0.2	1.04		0.60
^{245}Pu	Present work	5.40	1.93	5.00	0.80	1.00	0.52
(*e-o*)	Recommended	5.6±0.2		5.0±0.2	0.80		0.52
^{239}Am	Present work	6.40	2.10	5.22	0.80	1.00	0.52
(*o-e*)	Recommended	6.2±0.3		5.60	0.80		0.52
^{240}Am	Present work	6.50	2.30	5.70	0.65	1.00	0.45
(*o-o*)	Recommended	6.5±0.2		5.2±0.3	0.65		0.45
^{241}Am	Present work	6.00	1.70	5.05	0.80	1.00	0.52
(*o-e*)	Recommended	6.0±0.2		5.1±0.3	0.80		0.52
^{242}Am	Present work	6.78	2.20	5.78	0.65	1.00	0.45
(*o-o*)	Recommended	6.5±0.2		5.4±0.3	0.65		0.45
^{243}Am	Present work	5.80	1.80	5.20	0.80	1.00	0.52
(*o-e*)	Recommended	5.9±0.2		5.4±0.3	0.80		0.52
^{244}Am	Present work	6.50	2.30	5.70	0.65	1.00	0.45
(*o-o*)	Recommended	6.3±0.2		5.4±0.3	0.65		0.45
^{245}Am	Present work	5.90	2.10	5.335	0.80	1.00	0.52
(*o-e*)	Recommended	5.9±0.2		5.2±0.3	0.80		0.52
^{241}Cm	Present work	6.60	1.60	4.52	0.80	1.00	0.52
(*e-o*)	Recommended	6.3±0.3		4.3±0.5	0.80		0.52
^{242}Cm	Present work	5.70	1.27	4.00	1.04	1.00	0.60
(*e-e*)	Recommended	5.8±0.4		4.0±0.5	1.04		0.60
^{243}Cm	Present work	6.70	1.40	4.40	0.80	1.00	0.52
(*e-o*)	Recommended	6.4±0.3		4.30	0.80		0.52
^{244}Cm	Present work	5.60	1.67	4.20	1.04	1.00	0.60
(*e-e*)	Recommended	5.8±0.2		4.3±0.3	1.04		0.60
^{245}Cm	Present work	6.00	1.90	4.80	0.80	1.00	0.52
(*e-o*)	Recommended	6.2±0.2		5.00	0.80		0.52

the actinide nuclides listed in Table II, the parabolic parametrization leads to consistently higher values for the spontaneous fission half-lives than those calculated using the third-degree polynomials with the last part of the fission barrier (beyond the second saddle) approximated by a straight line. Such differences are seen to lie approximately between two and five orders of magnitude depending on the nature of the fissioning nucleus. The even-even nuclei show the least discrepancies of approximately one to two orders of magnitude. However, such differences are seen to increase considerably to approximately five orders of magnitude for the doubly odd nuclei with the results for the odd-A nuclei lying somewhere between these extremes. Such differences in the calculated fission half-lives can be understood in terms of a comparison of such suitably parametrized shapes for these nuclei, as shown in Fig. 5.

We observe that the double-humped fission barrier parametrized using the third-degree polynomials (b) to connect the successive extremum points leads consistently to the smallest possible values of the calculated fission half-lives among the various different potential parametrizations considered in the present work. Such a path therefore seems to minimize the action integral so as to yield the maximum value of the fission penetrability at the ground state among the various different parametrizations considered here. The parameters listed in Table I were obtained earlier by Bhandari[22] in an attempt to test the simultaneous consistency of the smoothly joined parabolic parametrization with a number of fission observables such as the near-barrier fission cross sections, isomeric fission half-lives and branching ratios, and the ground-state spontaneous fission half-lives for a wide variety of 25 actinide nuclei. While a good agreement on even-even nuclei was found in that work, the calculation predicted too large spontaneous fission half-lives for the odd-A and for the doubly odd nuclei as compared with their measured values. Such differences are seen to be lowered when third-degree polynomials (b) are used to parametrize the double-humped fission barrier as apparent from the general trend of the calculated results displayed in Table II. The experimental results listed in Table II were taken from their compilation by Vandenbosch and Huizenga in their text[27] on nuclear fission, and have been updated, where necessary, to be compatible with those listed in the most recent review paper on spontaneous fission by Hoffman and Sommerville.[28]

For most of the even-even nuclei, the spontaneous fission half-lives as obtained in the third-degree polynomials (b) parametrization are seen (Table II) to be somewhat smaller than their measured values. This can be corrected by constructing the last part of the barrier us-

TABLE II. Comparison of the ground-state spontaneous fission half-lives calculated using the various different parametrizations of the double-humped fission barrier for the 25 actinide nuclei listed in Table I. Measured values of the corresponding half-lives are also listed.

		Ground-state spontaneous fission half-lives (yr) Calculated results using the double-humped fission barrier parametrized by				
Compound nucleus	Even-odd character of Z-N	smoothly joined parabolic segments	third-order polynomials (a)	third-order polynomials (b)	straight lines	Measured values
^{236}U	*e-e*	3.85×10^{16}	9.73×10^{16}	1.33×10^{15}	4.92×10^{15}	2×10^{16}
^{238}U	*e-e*	1.10×10^{15}	7.41×10^{14}	9.16×10^{12}	3.85×10^{13}	6×10^{15}
^{237}Np	*o-e*	4.29×10^{19}	3.50×10^{18}	2.50×10^{16}	9.73×10^{16}	$>10^{18}$
^{235}Pu	*e-o*	9.43×10^{18}	7.68×10^{17}	7.06×10^{15}	2.77×10^{16}	
^{237}Pu	*e-o*	8.53×10^{19}	5.85×10^{18}	5.01×10^{16}	2.06×10^{17}	
^{238}Pu	*e-e*	1.46×10^{11}	1.21×10^{11}	2.22×10^{9}	7.54×10^{9}	$(5\pm0.6)\times10^{10}$
^{239}Pu	*e-o*	4.62×10^{22}	2.75×10^{21}	1.53×10^{19}	7.26×10^{19}	5.5×10^{15}
^{240}Pu	*e-e*	4.14×10^{11}	3.06×10^{11}	5.61×10^{9}	2.07×10^{10}	1.2×10^{11}
^{241}Pu	*e-o*	4.76×10^{21}	2.20×10^{20}	1.89×10^{18}	9.21×10^{18}	$\sim6\times10^{16}$
^{242}Pu	*e-e*	2.92×10^{11}	2.29×10^{11}	3.82×10^{9}	1.37×10^{10}	7.5×10^{10}
^{243}Pu	*e-o*	2.07×10^{18}	1.60×10^{17}	1.66×10^{15}	6.58×10^{15}	
^{244}Pu	*e-e*	9.31×10^{10}	7.32×10^{10}	1.39×10^{9}	4.7×10^{9}	$(6.5\pm0.3)\times10^{10}$
^{245}Pu	*e-o*	1.55×10^{17}	1.17×10^{16}	1.19×10^{14}	4.77×10^{14}	
^{239}Am	*o-e*	9.64×10^{21}	5.69×10^{20}	4.97×10^{18}	1.99×10^{19}	
^{240}Am	*o-o*	1.72×10^{33}	6.52×10^{30}	1.54×10^{28}	8.81×10^{28}	
^{241}Am	*o-e*	1.52×10^{20}	8.43×10^{18}	8.31×10^{16}	3.6×10^{17}	$(2.3\pm0.8)\times10^{14}$
^{242}Am	*o-o*	1.88×10^{35}	4.88×10^{32}	1.07×10^{30}	6.52×10^{30}	$>3\times10^{12}$
^{243}Am	*o-e*	1.24×10^{20}	7.42×10^{18}	6.3×10^{16}	2.98×10^{17}	$(2\pm0.5)\times10^{13}$
^{244}Am	*o-o*	1.72×10^{33}	6.32×10^{30}	1.50×10^{28}	8.54×10^{28}	
^{245}Am	*o-e*	4.94×10^{20}	3.11×10^{19}	2.37×10^{17}	1.04×10^{18}	
^{241}Cm	*e-o*	4.57×10^{19}	2.38×10^{18}	3.79×10^{16}	2.20×10^{17}	
^{242}Cm	*e-e*	3.72×10^{7}	3.16×10^{7}	1.31×10^{6}	4.63×10^{6}	7.2×10^{6}
^{243}Cm	*e-o*	4.38×10^{19}	1.88×10^{18}	3.39×10^{16}	2.24×10^{17}	
^{244}Cm	*e-e*	5.70×10^{7}	5.18×10^{7}	1.96×10^{6}	5.66×10^{6}	1.4×10^{7}
^{245}Cm	*e-o*	2.76×10^{18}	1.90×10^{17}	2.44×10^{15}	9.04×10^{15}	$(1.4\pm0.2)\times10^{12}$

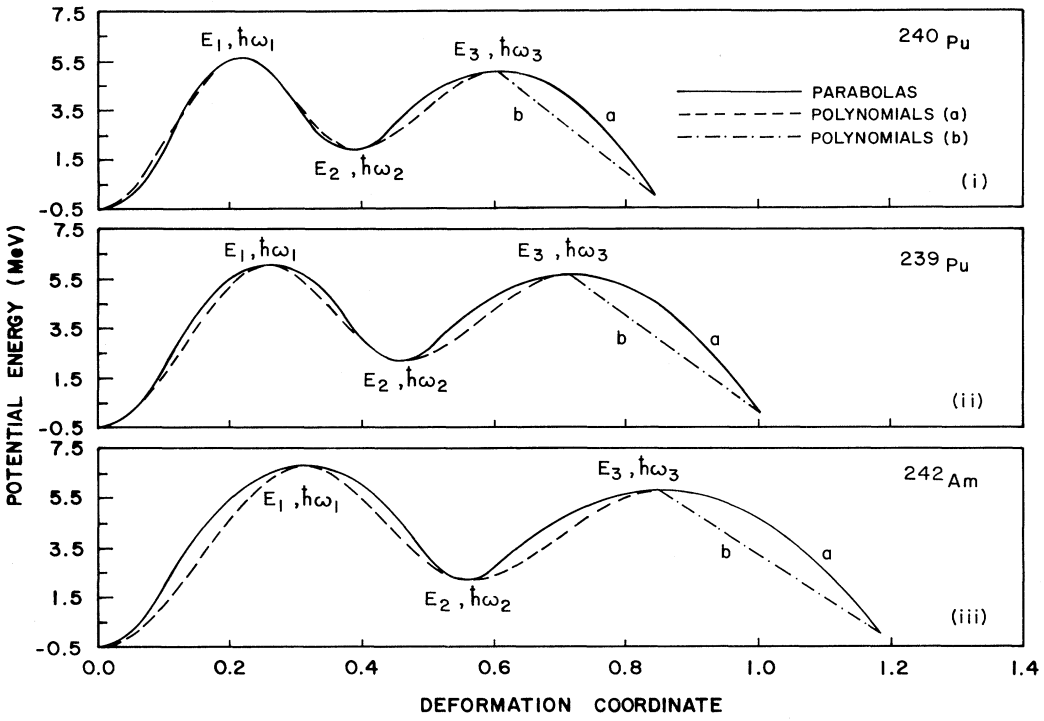

FIG. 5. Comparison of the double-humped fission barrier shapes parametrized using the smoothly joined parabolas and the third-degree polynomials for a typical (i) even-even nucleus, (ii) the odd-A nucleus, and (iii) the doubly odd nucleus. The corresponding barrier parameters of the smoothly joined parabolic segment potentials are (i) $E_0=-0.5$ MeV, $\hbar\omega_0=1.0$ MeV, $E_1=5.57$ MeV, $\hbar\omega_1=1.04$ MeV, $E_2=1.90$ MeV, $\hbar\omega_2=1.0$ MeV, $E_3=5.07$ MeV, $\hbar\omega_3=0.60$ MeV. (ii) $E_0=-0.5$ MeV, $\hbar\omega_0=1.0$ MeV, $E_1=6.0$ MeV, $\hbar\omega_1=0.80$ MeV, $E_2=2.20$ MeV, $\hbar\omega_2=1.0$ MeV, $E_3=5.65$ MeV, $\hbar\omega_3=0.52$ MeV. (iii) $E_0=-0.5$ MeV, $\hbar\omega_0=1.0$ MeV, $E_1=6.78$ MeV, $\hbar\omega_1=0.65$ MeV, $E_2=2.20$ MeV, $\hbar\omega_2=1.0$ MeV, $E_3=5.78$ MeV, $\hbar\omega_3=0.45$ MeV. Curves a and b beyond the second saddle have the same meanings as in Fig. 1.

ing a straight line from the second saddle to a point somewhat beyond the exit point, as already considered by some authors[7,8] in the past in the fission literature. It is important to note, however, that such a procedure introduces some arbitrariness or ambiguity in the parametrization of the double-humped fission barrier.

V. INERTIAL-MASS FUNCTION

It seems appropriate here to include also a brief discussion of the effect of the inertial-mass parameter and of its variation with the deformation (fission) coordinate on the fission penetrability and consequently on the calculated spontaneous fission half-lives of the actinide nuclei. In the present work we have assumed the mass parameter μ to be constant for all values of the dimensionless deformation parameter ϵ, and have given it the value as in Eq. (2). In the smoothly joined parabolic parametrization of the double-humped fission barrier, the mass parameter enters both in the potential parametrization [Eq. (1)] as well as in the action integral [Eqs. (10) and (11)] while calculating the fission penetrability or the fission half-lives. As long as μ is taken to be independent of ϵ, the inertial-mass parameter drops out[16] in the expression for the fission penetrability, and its only purpose is to scale the potential energy of deformation along the fission coordinate. Thus in the smoothly joined parabolic parametrization of the double-humped potential barrier, the fission penetrability function and consequently the fission half-lives are independent of the exact numerical value of μ as long as it is taken to be constant for all values of ϵ. On the other hand, the inertial-mass parameter does not enter explicitly into the potential parametrization when we construct the double-humped fission barrier using the third-degree polynomials or straight-line segments connecting the successive extremum points. Using such potential parametrizations the inertial mass therefore enters explicitly only in the action integral, as seen for example in Eqs. (10) and (11), while calculating the fission penetrability and will thus directly influence the calculated fission half-lives.

Inertial-mass functions and their dependence on the relevant fission coordinates have been obtained microscopically using the cranking model. Such calculations yield a fluctuating inertial mass reflecting the specific single-particle structure of the particular nucleus under consideration. However, different microscopic models yield very different results for the inertia, and are thus not completely reliable in their detailed calculation of the inertial-mass functions. Because of the uncertainties in

and the complexities of the microscopic models for the inertia, it has been found more advantageous to use the semiempirical approach to determine the inertial-mass functions. Using the third-degree polynomial parametrization of the double-humped fission barrier passing through the theoretically calculated extremum points along a selected one-dimensional path through the multidimensional potential-energy surface in fission, Randrup *et al.*[6,7] have obtained a semiempirical expression for the effective-inertial mass as a function of the deformation (fission) coordinate so as to reproduce the observed spontaneous fission half-lives of a variety of the actinide nuclei. Such a semiempirically determined mass parameter is found to decrease as a function of the fission coordinate until it approaches the asymptotic value equal to the reduced mass of the resulting fission fragments. In view of the large differences obtained in the present work in the calculated fission penetrability and in fission half-lives using different parametrizations of the double-humped fission barrier, it is important to realize that such empirically determined mass parameters may also depend somewhat on the particular mode of the potential parametrization.

VI. DISCUSSION AND CONCLUSIONS

The aim of the present work was to get some quantitative estimates of the ambiguity caused by the choice of different paths passing through the same extremum points along the fission direction. For this we have parametrized the double-humped fission barrier in various different ways using the smoothly joined parabolic segments, third-degree polynomials, and straight lines. The parametrization using straight lines to connect successive extremum points is obviously not much of physical interest as the resulting shapes are far from those expected in reality. Such parametrization was therefore included only for the purpose of comparison. The other two parametrizations lead to reasonably realistic and smoothly varying potential shapes as discussed earlier in the text. Using such parametrized shapes, we have also calculated the fission penetrability and the fission half-lives for a variety of actinide nuclei and have discussed the corresponding results and their comparison in the preceding sections.

The most significant result to emerge from this investigation is that while the parametrizations using the third-degree polynomials (b) and straight lines, respectively, lead to similar results (within an order of magnitude) on the fission penetrability and fission half-lives, the corresponding results using smoothly joined parabolic segment parametrization differ significantly by almost two to five orders of magnitude depending on the type of the nucleus and on the parameters of its corresponding double-humped barrier. The smoothly joined parabolic parametrization consistently leads to higher values for the fission half-lives for all the nuclei considered in the present work as compared to those obtained for the third-degree polynomials (b) parametrization. This result is in sharp contradiction with the conventional wisdom currently prevalent in fission literature,[8] holding that selecting different potential parametrizations or fission paths passing through the same extremum points does not affect the calculated fission half-lives by more than an order of magnitude. Fission penetrability and fission half-lives are both known to be extremely sensitive to the heights of the fission barriers relative to the ground state of the fissioning nucleus. However, the differences that we have attempted to delineate in the present work are in addition to the dependence of the fission half-lives on such barrier heights or on the ground-state energy.

In the absence of any exact knowledge of the fission path that nature selects for a given fissioning nucleus, it would be an entirely futile attempt on our part to recommend one over the other potential parametrization for the double-humped fission barrier. It is, however, meaningful here to summarize the merits and limitations as well as their relevance to the various fission observables of the two realistic potential parametrizations, namely, those using the smoothly joined parabolic segments and the third-degree polynomials, respectively. Smoothly joined parabolic segments have been commonly used in fission literature to parametrize the double-humped fission barrier to analyze various types of near- and subbarrier fission data obtained in a variety of experiments. Quantitative information on the parameters of such a parametrized fission barrier can be obtained from the various fission observables as summarized recently by Weigmann.[29] For example, the fission "threshold," i.e., the energy at which the fission probability rises quickly, yields rather accurate information on the height of the higher of the two barriers. The slope of the fission penetrability (cross section) near threshold depends[20] on the value of the parameter $\hbar\omega$ of the higher barrier. Finally, the plateau value of the cross section above the fission threshold depends on the height of the lower barrier. Similarly, the experimentally measured information on the energies and half-lives of the fission isomers and of their excited states (vibrational resonances) helps determine the parameters of the second well in a double-humped barrier parametrized using the smoothly joined parabolic segments. For a given set of the predetermined heights of the two barriers, the overall width of the double-humped fission barrier is then directly related to the spontaneous fission half-life from the ground state of a fissioning compound nucleus.

In view of such an intimate correspondence with the various fission observables, it is not surprising that fairly accurate information on various parameters of the double-humped fission barriers parametrized using the smoothly joined parabolic segments has been accumulated over the past three decades. An extensive quantitative analysis carried out by Bjørnholm and Lynn has resulted in the most accurate quantitative information available so far on the various parameters of the double-humped fission barrier for most of the actinides as summarized in their review paper.[5] Such a potential parametrization also does not require the exact locations of the various extremum points on the fission path along the deformation axis. However, as shown clearly in the present work, such a parametrization consistently underestimates the fission penetrability and thereby predicts consistently

higher values of the fission half-lives.

The use of third-degree polynomials in parametrizing the double-humped fission barrier has so far been restricted only to the theoretical calculations of fission half-lives. The results of the present work show that this method, in particular the third-degree polynomials (b) parametrization, leads to the smallest possible values of the calculated spontaneous fission half-lives among the various different potential parametrizations considered by us. Such a procedure therefore seems to minimize the action integral resulting in the largest value of the fission penetrability as compared with the other parametrizations. However, this method of potential parametrization suffers from a serious limitation in that it requires an exact knowledge of the locations of the various extremum points on the fission path along the deformation axis. No such accurate information can so far be obtained from fission experiments. The various spectroscopic properties of the fission isomers revealing their large deformation relative to that of the ground state of the corresponding fissioning compound nucleus, such as moments of inertia and quadrupole moments, lead only to approximate quantitative estimates and cannot thus be used to parametrize accurately the corresponding double-humped fission barrier using the third-degree polynomials to connect the successive extremum points. The biharmonic nature of the potential shapes near the extremum points, as obtained in such a potential parametrization, may also preclude any close correspondence between its parameters and the various fission observables.

The authors wish to thank Dr. M. El-Fazzani, Dr. S. N. Soni, and Ali Al-Kharam for their interest in this work.

---

*Present address: Experimental Physics Division, Atomic Research Centre, The Bangladesh Atomic Energy Commission, P.O. Box 164, Dacca, Bangladesh.

[1]V. M. Strutinsky, Nucl. Phys. **A95**, 420 (1967); **A122**, 1 (1968).
[2]J. R. Nix, Annu. Rev. Nucl. Sci. **22**, 65 (1972).
[3]M. Brack, J. Damgaard, H. C. Pauli, A. S. Jensen, V. M. Strutinsky, and C. Y. Wong, Rev. Mod. Phys. **44**, 320 (1972).
[4]H. J. Specht, Rev. Mod. Phys. **46**, 773 (1974).
[5]S. Bjørnholm and J. E. Lynn, Rev. Mod. Phys. **52**, 725 (1980).
[6]J. Randrup, C. F. Tsang, P. Möller, S. G. Nilsson, and S. E. Larsson, Nucl. Phys. **A217**, 221 (1973).
[7]J. Randrup, S. E. Larsson, P. Möller, S. G. Nilsson, K. Pomorski, and A. Sobiczewski, Phys. Rev. C **13**, 229 (1976).
[8]P. Möller, J. R. Nix, and W. J. Swiatecki, Nucl. Phys. **A469**, 1 (1987); **A492**, 349 (1989).
[9]K. Boning, Z. Patyk, A. Sobiczewski, and S. Ĉwiok, Z. Phys. A **325**, 479 (1986).
[10]S. Ĉwiok, P. Rozmej, A. Sobiczewski, and Z. Patyk, Nucl. Phys. **A491**, 281 (1989).
[11]Z. Patyk, J. Skalski, A. Sobiczewki, and S. Ĉwiok, Nucl. Phys. **A502**, 591c (1989).
[12]D. R. Inglis, Phys. Rev. **96**, 1059 (1954); **97**, 701 (1955).
[13]A. Sobiczewski, Fiz. Elem. Chastits At. Yadra **10**, 1170 (1979) [Sov. J. Part. Nucl. **10**, 446 (1979)].
[14]J. Kunz and J. R. Nix, Nucl. Phys. **A426**, 353 (1984).
[15]J. R. Nix and G. E. Walker, Nucl. Phys. **A132**, 60 (1969).
[16]J. D. Cramer and J. R. Nix, Phys. Rev. C **2**, 1048 (1970).
[17]B. S. Bhandari, Ph.D. thesis, Ohio University, 1974.
[18]B. S. Bhandari, Phys. Rev. C **19**, 1820 (1979); **22**, 606 (1980).
[19]B. S. Bhandari and A. S. Al-Kharam, University of Garyounis report, 1986 (unpublished), and the references cited therein.
[20]B. S. Bhandari and A. S. Al-Kharam, Phys. Rev. C **39**, 917 (1989).
[21]B. S. Bhandari and F. Zamani-Noor (unpublished).
[22]B. S. Bhandari, Phys. Rev. C **42**, 1443 (1990).
[23]E. W. Gettys and H. W. Graben, Am. J. Phys. **43**, 625 (1975).
[24]M. Prakash, J. Phys. A **9**, 1847 (1976).
[25]N. Fröman and P. O. Fröman, *JWKB Approximation* (North-Holland, Amsterdam, 1965), pp. 90–101.
[26]R. W. Hamming, *Introduction to Applied Numerical Analysis* (McGraw-Hill, New York, 1971).
[27]R. Vandenbosch and J. R. Huizenga, *Nuclear Fission* (Academic, New York, 1973).
[28]D. C. Hoffman and L. P. Somerville, in *Particle Emission from Nuclei, Vol. III [Fission and Beta-delayed Decay Modes]*, edited by D. N. Poenaru and M. S. Ivascu (CRC, Boca Raton, Florida, 1988), p. 1.
[29]H. Weigman, in *Proceedings of the International Conference on 50 Years with Nuclear Fission, National Institute of Standards and Technology, Gaithersburg, Maryland, 1989,* edited by J. W. Behrens and A. D. Carlson (American Nuclear Society, La Grange Park, Illinois, 1989), p. 168.